Physics Letters A 376 (2012) 1465–1467

Contents lists available at SciVerse ScienceDirect

Physics Letters A

www.elsevier.com/locate/pla

Coalescence of B_nN_n fullerenes: A new pathway to produce boron nitride nanotubes with small diameter

Yongliang Yong, Kai Liu, Bin Song *, Pimo He, Peng Wang, Hongnian Li

State Key Laboratory of Silicon Materials and Department of Physics, Zhejiang University, Hangzhou 310027, People's Republic of China

ARTICLE INFO

Article history:
Received 5 January 2012
Accepted 5 March 2012
Available online 8 March 2012
Communicated by R. Wu

Keywords:
B_nN_n fullerenes
Coalescence
BN nanotubes
Density functional theory calculations

ABSTRACT

Using density functional theory calculations, we predict that single-walled hemispherical-caped boron nitride (BN) nanotubes with small diameters can be produced via the coalescence of stable nanoclusters. Specifically, the assembly of B_nN_n ($n = 12, 24$) clusters exhibiting particularly high stability and leading to armchair (3, 3) and (4, 4) BN nanotubes, respectively, are considered. The formed finite-length BN nanotubes have semiconducting properties with wide band gaps attractive to nano-device applications.

1. Introduction

After its successful experimental realization [1], carbon nanotubes (CNTs) have stimulated tremendous interest in the extraordinary properties of nanotubular structures [2]. Recently, boron nitride nanotubes (BNNTs), which are structurally similar to CNTs, have attracted increasing attention [3–8]. BNNTs were theoretically predicted [9] in 1994 and successfully synthesized in 1995 [10]. Compared with metallic or semiconducting CNTs, BNNTs are all stable wide band gap semiconductors independent of their helicity and diameter, regardless of whether the nanotube is single-walled or multi-walled [8]. In addition, BNNTs possess high chemical stability, excellent mechanical properties, and high thermal conductivity [5]. Thus, BNNTs are expected to be a promising nanomaterial in a variety of potential fields such as nano-devices, functional composites, and electrically insulating substrates [5,11].

Nowadays, research on CNTs has become popular because many laboratories are capable of producing their own samples for various investigations. However, the progress of BNNT research is still limited by the availability of BNNT samples for widespread investigation of their properties and applications. The techniques known for BNNT growth, for example, arc-discharge [10], laser vaporization [12], BN substitution method from CNT templates [13], chemical vapor deposition (CVD) [14], and high-temperature ball milling [15], involve either specific instrumentation, high growth temperatures (>1300°C), and/or dangerous chemistry. Recently, despite the low-temperature synthesis of BNNTs, such as plasma-enhanced pulsed-laser deposition (PE-PLD) [16], high-quality BNNT samples still remained difficult to produce. Furthermore, growing highly pure single-walled BNNTs remains a challenge, especially for small diameter BNNTs [7]. To date, a number of theoretical works have predicted the existence of BNNTs with small diameters (e.g., see Ref. [9]) and possibly possessing semiconducting properties with direct or indirect band gaps. However, there are few experimental reports on the synthesis of this kind of BNNT; only the zigzag (6, 0) BNNT with a small diameter of 5 Å has been reported [17]. This hinders new understanding of the properties of BNNTs and the promotion of research in the field.

On the other hand, small CNTs with diameters of 7 [18], 5 [19], and 4 Å [20,21] are reportedly associated with C_{60}, C_{36}, and C_{20} fullerenes, respectively. This consistency is expected to be valid for BNNTs as well. BN fullerenes have been predicted theoretically [22–26], and B_nN_n fullerenes with $n = 12$–60 have been synthesized successfully [27–31]. These B_nN_n fullerenes could be assembled in other nanoporous BN nanomaterials [32–34].

In this Letter, our initial, promising results are presented to show the possibility of producing BNNTs with small diameters by coalescing small B_nN_n fullerenes at room temperature. In the current work, $B_{12}N_{12}$ and $B_{24}N_{24}$ fullerenes are selected as examples.

2. Computational methods

All calculations are performed using the spin-polarized density functional theory (DFT) implemented in the DMOL^3 program (Accelyrs, Inc.) [35,36]. The generalized gradient approximation formulated by Perdew, Burke, and Ernzerhof (PBE) [37] is employed to describe the exchange-correlation energy functional. All-electron core treatment and double numerical basis set

* Corresponding author. Tel./fax: +86 571 87951328.
E-mail address: bzsong@css.zju.edu.cn (B. Song).

0375-9601/$ – see front matter
doi:10.1016/j.physleta.2012.03.011

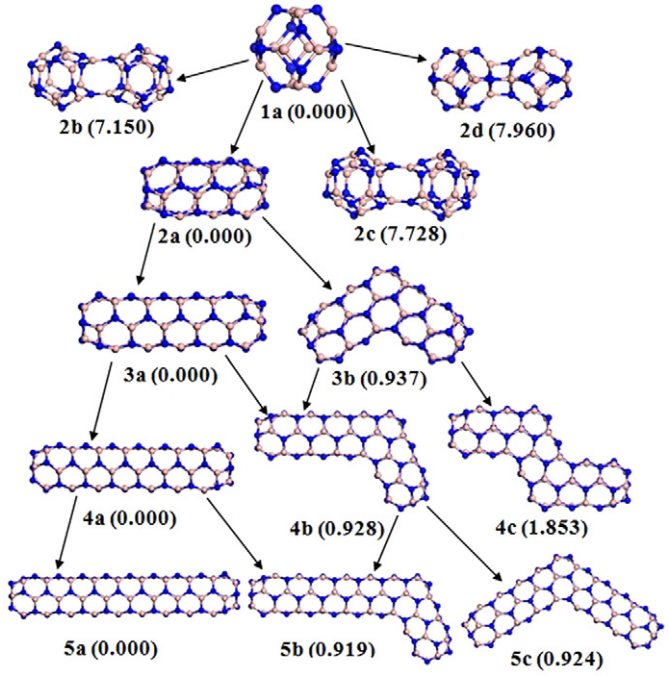

Fig. 1. The evolution of the geometrical structures of $(B_{12}N_{12})_m$ $(m = 1–5)$ coalescences. Isomeric structures of $(B_{12}N_{12})_m$ coalescences are labeled as *ma*, *mb*, *mc*, etc in order of decreasing stability for each coalescence size *m*. Here and in the following figures, values in parentheses are relative energies with respect to the most stable isomer for each composition in eV. The blue balls represent B atoms and the pink balls represent N atoms. (For interpretation of the references to color in this figure legend, the reader is referred to the web version of this Letter.)

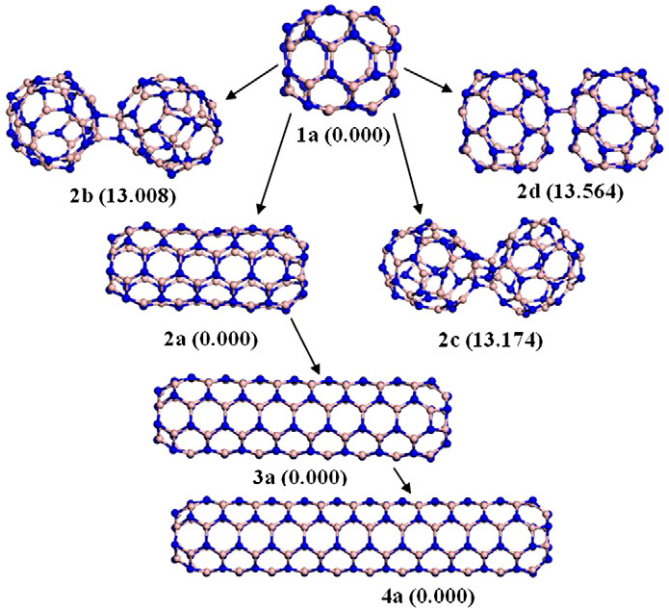

Fig. 2. The evolution of the geometrical structures of $(B_{24}N_{24})_m$ $(m = 1–4)$ assemblies. Isomeric structures of $(B_{24}N_{24})_m$ assemblies are labeled as *ma*, *mb*, *mc*, and so on in order of decreasing stability for each assembly size *m*.

supplemented with *d*-polarization functions (i.e., the DNP set) are selected. Self-consistent field procedures are performed with a convergence criterion of 10^{-6} a.u. on the energy and electron density. The geometries are fully optimized without any symmetry constraints. We use a convergence criterion of 10^{-3} a.u. on the gradient and displacement and 10^{-5} a.u. on the total energy in geometrical optimizations. Such energy tolerances and maximum force are small enough to ensure the establishment of actual equilibrium structures. Normal-mode vibrational analysis is applied to guarantee that the optimized geometries are real local minima. The results of a vibrational analysis calculation are used to compute important thermodynamic properties such as enthalpy (H), entropy (S) and free energy (G) at finite temperature.

3. Results and discussion

We begin the investigation by confirming the structural and electronic properties of B_nN_n $(n = 12, 24)$ fullerenes. Figs. 1(1a) and 2(1a) show the optimized equilibrium configurations of $B_{12}N_{12}$ and $B_{24}N_{24}$, respectively. $B_{12}N_{12}$ fullerene is found to be highly stable at a spherical cage structure with high symmetry (T_h), consisting of six isolated four-membered rings (4MRs) and eight six-membered rings (6MRs). The $B_{12}N_{12}$ fullerene is regarded as the smallest volume cluster obeying the law of isolated 4MRs (an analog of the law of isolated pentagons for the buckminsterfullerene C_{60}), which serves as a criterion for its stability. The energy gap between the highest occupied (HOMO) and lowest unoccupied (LUMO) molecular orbitals for the $B_{12}N_{12}$ fullerene is 5.055 eV, an indication of its semiconducting properties. The $B_{24}N_{24}$ fullerene with S_8 symmetry, which contains two eight-membered rings (8MRs), eight isolated 4MRs, and sixteen 6MRs, is found to be the most energetically favorable cage structure. The two isolated 8MRs are located at the ends of the cage. Furthermore, the HOMO–LUMO gap value for the $B_{24}N_{24}$ fullerene is 4.723 eV. Our calculated results are in complete agreement with the previous theoretical and experimental studies on B_nN_n $(n = 12, 24)$ fullerenes [22–31].

Subsequently, the initial growth behavior of the coalescence of B_nN_n $(n = 12, 24)$ fullerenes are considered. Figs. 1 and 2 show the evolutions of the optimized geometrical structures of $(B_{12}N_{12})_m$ and $(B_{24}N_{24})_m$ $(m = 1–5)$ coalescences, respectively. In the present study, all possible dimer interactions are checked. The coalescence of two $B_{12}N_{12}$ cages is energetically favorable, resulting in structurally stable products [see Fig. 1(2a–2d)]. However, the 6MR face coalescence of two $B_{12}N_{12}$ cages, the full optimization of which leads to a tubular $B_{24}N_{24}$ cluster (isomer 2a), is the most energetically favorable among the coalescences. The most stable isomer 2a of $B_{12}N_{12}$ dimers is, at least, 7.150 eV lower in energy with respect to the other dimeric isomers. This indicates that the system may result in a big minimum of potential energy surface during the 6MR face coalescence. Matxain et al. [32] also reported that the 6MR face coalescence of $B_{12}N_{12}$ cages results in a condensed $B_{24}N_{24}$ cluster. Due to the great differences in energy between the 6MR face coalescence and others, we only consider the 6MR face coalescence below when more $B_{12}N_{12}$ cages are brought together. Fig. 1(3a and 3b) shows two lowest-energy structures of $B_{12}N_{12}$ trimers. The tubular motif is found to be the most stable structure. The second structure with the bent tubular motif is only higher above 0.937 eV in energy. To further determine the geometric features of $(B_{12}N_{12})_m$ coalescences, the geometries of $(B_{12}N_{12})_4$ are tested. Bringing four $B_{12}N_{12}$ cages together, the tubular motif is found to still be preferable, energetically, to the bent tubular motif. As the number of $B_{12}N_{12}$ monomer increases, the tubular feature continues as shown in Fig. 1. Considering the lowest-energy of the coalescence process, we may understand a continuation of this coalescence process to form an armchair $(3, 3)$ BN nanotube with hemispherical caps. The armchair $(3, 3)$ BN nanotube has a small diameter of approximately 4.14 Å.

The coalescence of $B_{24}N_{24}$ fullerenes is similar to the case of $B_{12}N_{12}$ coalescence, as shown in Fig. 2. The 8MR face coalescence is more favorable, energetically, than the other coalescences. For dimers, the tubular structure is the lowest-energy form, which is at least 13.008 eV lower in energy than the other coalescences. The tubular structure continues because of the great difference in

Table 1
The binding energy per BN (E_b), free energy difference (ΔG),[a] and energy gap (E_g) for the most stable structures of B_nN_n coalescences and corresponding BNNTs.

System	E_b (eV)	ΔG (eV)	E_g (eV)
$B_{12}N_{12}$	12.687		5.055
$(B_{12}N_{12})_2$	13.100	−9.004	4.656
$(B_{12}N_{12})_3$	13.238	−8.992	4.529
$(B_{12}N_{12})_4$	13.307	−8.915	4.463
$(B_{12}N_{12})_5$	13.348	−9.042	4.421
(3, 3) BNNT	13.451		4.44
$B_{24}N_{24}$	13.169		4.723
$(B_{24}N_{24})_2$	13.463	−9.453	4.512
$(B_{24}N_{24})_3$	13.564	−16.936	4.390
$(B_{24}N_{24})_4$	13.614	−13.357	4.330
(4, 4) BNNT	13.756		4.40

[a] The free energy difference for the coalescence channel "$(B_nN_n)_{m-1} + B_nN_n \rightarrow (B_nN_n)_m$" at room temperature is defined by $\Delta G(T) = \Sigma\Delta G_{product}(T) - \Sigma\Delta G_{reactant}(T)$.

energy among the isomers. An armchair (4, 4) BN nanotube with a small diameter of 5.47 Å can be formed by the 8MR face coalescence of $B_{24}N_{24}$ cages. The number of $B_{24}N_{24}$ cages evidently determines the length of the tube.

The calculated binding energy per BN (E_b) of the most stable B_nN_n ($n = 12, 24$) assemblies is shown in Table 1. The E_b is defined by $E_b = (nE_B + nE_N - E_{BN})/n$, where E_B and E_N are the total energies of an isolated B and N atom, respectively; E_{BN} is the total energy of the corresponding B_nN_n system; and n is the number of B or N atoms involved. For each B_nN_n ($n = 12, 24$) assembly, the E_b is found to increase smoothly with the increase of assembly size m, indicating that the $(B_{12}N_{12})_m$ and $(B_{24}N_{24})_m$ assemblies would be more stable than the $(B_{12}N_{12})_{m-m'}$ and $(B_{24}N_{24})_{m-m'}$ ($m > m'$) assemblies, respectively. Based on Table 1, the E_b of BNNTs is clearly only a little larger than that of the corresponding B_nN_n assembly with finite size. This may confirm that armchair hemispherical-caped BNNTs with small diameters could be formed by coalescing B_nN_n fullerenes. To understand the stability of B_nN_n fullerene coalescences and its feasibility further, the free energy differences of the coalescence process at room temperature are calculated. The results are listed in Table 1. The free energy differences for the most stable $(B_nN_n)_m$ coalescences are all negative, indicating that these coalescences are energetically favorable and that the coalescence process will occur spontaneously at room temperature.

The HOMO–LUMO gaps for the most stable structures are calculated to gain further understanding of the properties of the B_nN_n fullerenes' coalesced structures. The results are listed in Table 1. The HOMO–LUMO gaps are sensitive to the assembly size. The magnitude of the gaps varies from 4.330 to 5.055 eV, indicating that the finite-size B_nN_n assemblies with round-capped tubular structures have semiconducting properties. From the point of view of developing BN-based nanostructures, the discussed semiconducting behaviors of finite BN nanotubes are very interesting for nano-device applications.

4. Conclusions

In summary, using density functional theory calculations, we report theoretical evidence of the formation of single-walled hemispherical-caped BN nanotubes with small diameters via the coalescence of B_nN_n ($n = 12, 24$) fullerenes. The coalescence process is an energetically efficient pathway to form small BN nanotubes with hemispherical caps at room temperature. The coalescence of $B_{12}N_{12}$ fullerenes produces an armchair (3, 3) BN nanotube with a small diameter of approximately 4.14 Å. The coalescence of $B_{24}N_{24}$ fullerenes results in an armchair (4, 4) BN nanotube with a diameter of 5.47 Å. Finite-sized BN nanotubes have semiconducting properties, an indication of their usefulness in nano-device applications. Hopefully, our results will stimulate experiments to produce these single-walled hemispherical-caped BNNTs with small diameters.

Acknowledgements

This work was supported by National Basic Research Program of China (973) under Grant No. 2010CB631304, the National Natural Science Foundation of China (No. 11074214), and the Ministry of Science and Technology of China.

References

[1] S. Iijima, Nature 354 (1991) 56.
[2] R. Saito, G. Dresselhaus, M. Dresselhaus, Physical Properties of Carbon Nanotubes, Imperial College Press, London, 1998.
[3] D. Golberg, Y. Bando, C.C. Tang, C.Y. Zhi, Adv. Mater. 19 (2007) 2413.
[4] R. Arenal, X. Blasé, A. Loiseau, Adv. Phys. 59 (2010) 101.
[5] D. Golberg, Y. Bando, Y. Huang, T. Terao, M. Mitome, C. Tang, C. Zhi, ACS Nano 4 (2010) 2979.
[6] J. Wang, C.H. Lee, Y.K. Yap, Nanoscale 2 (2010) 2028.
[7] C. Zhi, Y. Bando, C. Tang, D. Golberg, Mater. Sci. Eng. R 70 (2010) 92.
[8] P. Ayala, R. Arenal, A. Loiseau, A. Rubio, T. Pichler, Rev. Mod. Phys. 82 (2010) 1844.
[9] A. Rubio, J.L. Corkill, M.L. Cohen, Phys. Rev. B 49 (1994) 5081.
[10] N.G. Chopra, R.J. Luyken, K. Cherrey, V.H. Crespi, M.L. Cohen, S.G. Louie, A. Zettl, Science 269 (1995) 966.
[11] M. Radosavljević, J. Appenzeller, V. Derycke, R. Martel, P. Avouris, A. Loiseau, J. Cochon, D. Pigache, Appl. Phys. Lett. 82 (2003) 4131.
[12] R. Arenal, O. Stephan, J.L. Cochon, A. Loiseau, J. Am. Chem. Soc. 129 (2007) 16183.
[13] W. Han, Y. Bando, K. Kurashima, T. Sato, Appl. Phys. Lett. 73 (1998) 3085.
[14] M.J. Kim, S. Chatterjee, S.M. Kim, E.A. Stach, M.G. Bradley, M.J. Pender, L.G. Sneddon, B. Maruyama, Nano Lett. 8 (2008) 3298.
[15] Y. Chen, L.T. Chadderton, J.F. Gerald, J.S. Williams, Appl. Phys. Lett. 74 (1999) 2960.
[16] J. Wang, V.K. Kayastha, Y.K. Yap, Z. Fan, J.G. Lu, Z. Pan, I.N. Ivanov, A.A. Puretzky, D.B. Geohegan, Nano Lett. 5 (2005) 2528.
[17] E. Bengu, L.D. Marks, Phys. Rev. Lett. 86 (2001) 2385.
[18] P.M. Ajayan, S. Iijima, Nature 358 (1992) 23.
[19] L.F. Sun, S.S. Xie, W. Liu, W.Y. Zhou, Z.Q. Liu, D.S. Tang, G. Wang, L.X. Qian, Nature 403 (2000) 384.
[20] L.C. Qin, X.L. Zhao, K. Hirahara, Y. Miyamoto, Y. Ando, S. Iijima, Nature 408 (2000) 50.
[21] N. Wang, Z.K. Tang, G.D. Li, J.S. Chen, Nature 408 (2000) 50.
[22] R.J.C. Batista, M.S.C. Mazzoni, H. Chacham, Chem. Phys. Lett. 421 (2006) 246.
[23] R.R. Zope, T. Baruah, M.R. Pederson, B.I. Dunlap, Chem. Phys. Lett. 393 (2004) 300.
[24] L. Koponen, L. Tunturivuori, M.J. Puska, R.M. Nieminen, J. Chem. Phys. 126 (2007) 214306.
[25] S.S. Alexandre, H. Chacham, R.W. Nunes, Phys. Rev. B 63 (2001) 045402.
[26] S.A. Shevlin, Z.X. Guo, H.J.J. van Dam, P. Sherwood, C.R.A. Catlow, A.A. Sokol, S.M. Woodley, Phys. Chem. Chem. Phys. 10 (2008) 1944.
[27] D. Golberg, Y. Bando, O. Stéphan, K. Kurashima, Appl. Phys. Lett. 73 (1998) 2441.
[28] T. Oku, A. Nishiwaki, I. Narita, M. Gonda, Chem. Phys. Lett. 380 (2003) 620.
[29] D. Golberg, A. Rode, Y. Bando, M. Mitome, E. Gamaly, B. Luther-Davies, Diam. Relat. Mater. 12 (2003) 1269.
[30] T. Oku, I. Narita, A. Nishiwaki, Mater. Manuf. Process. 19 (2004) 1215.
[31] T. Oku, A. Nishiwaki, I. Narita, Sci. Technol. Adv. Mater. 5 (2004) 635.
[32] J.M. Matxain, L.A. Eriksson, J.M. Mercero, X. Lopez, M. Piris, J.M. Ugalde, J. Poater, E. Matito, M. Sola, J. Phys. Chem. C 111 (2007) 13354.
[33] A.V. Pokropivny, Diam. Relat. Mater. 15 (2006) 1492.
[34] S.S. Alexandre, R.W. Nunes, H. Chacham, Phys. Rev. B 66 (2002) 085406.
[35] B. Delley, J. Chem. Phys. 92 (1990) 508.
[36] B. Delley, J. Chem. Phys. 113 (2000) 7756.
[37] J.P. Perdew, K. Burke, M. Ernzerhof, Phys. Rev. Lett. 77 (1996) 3865.